

---

# Encoding High-Level Visual Attributes in Capsules for Explainable Medical Diagnoses

---

**Rodney LaLonde**

Center for Research in Computer Vision  
University of Central Florida  
Orlando, FL 32816  
lalonde@knights.ucf.edu

**Drew Torigian**

Department of Radiology  
University of Pennsylvania  
Philadelphia, PA 19104  
drew.torigian@penncmedicine.upenn.edu

**Ulas Bagci**

Center for Research in Computer Vision  
University of Central Florida  
Orlando, FL 32816  
bagci@crcv.ucf.edu

## Abstract

Deep neural networks are often called black-boxes due to their difficult-to-interpret decisions. This is characteristic of a deeper trend in machine learning, where predictive performance typically comes at the cost of *interpretability*. In some domains, such as image-based diagnostic tasks, understanding the reasons behind machine generated predictions is vital in assessing trust. In this study, we introduce novel designs of *capsule networks* to provide explainable diagnoses. Our proposed deep explainable capsule architecture, called *DX-Caps*, can encode high-level visual attributes within the vectors of capsules in order to simultaneously produce malignancy predictions for lung cancer as well as approximations of six visually-interpretable attributes, used by radiologists to explain their predictions. To reduce parameter and memory burden of this deeper network, we introduce a new capsule-average pooling function. With this simple, but fundamental addition, capsule networks can be designed in a deeper fashion than was possible before. Our overall approach can be characterized as multi-task learning; we learn to approximate the six high-level visual attributes of a lung nodule within the vectors of our uniquely constructed deep capsule network, while simultaneously segmenting the nodule and predicting its malignancy potential (diagnosis). Tested on over 1000 CT scans, our experimental results show that our proposed algorithm can approximate the visual attributes of lung nodules far better than a deep multi-path dense 3D CNN [1]. The proposed network also achieves higher diagnostic accuracy than a baseline explainable capsule network *X-Caps* and CapsNet [2] when applied to this task for the first time as well. To the best of our knowledge, this is the first study to investigate capsule networks for visual attribute prediction in general, and explainable medical image diagnosis in particular.

## 1 Introduction

Although deep learning (DL) has played a major role in a wide array of fields, there exist several which have yet to be comparably impacted: military, security, transportation, finance, legal, and healthcare among others [3, 4, 5]. At its core, DL owes its success to the joining of two essential tasks, *feature extraction* and *feature classification*, learned in a joint manner, usually through a form

of backpropagation. Although this direction has dramatically improved the predictive performance on a diverse range of tasks, it has also come at a great cost, the sacrifice of human-level *explainability*. As features become less *interpretable*, and the functions learned more complex, model predictions become more difficult to explain and the generalization ability of trained networks is less well understood. Several works have begun to press towards this goal of explainable deep learning, as explored in Section 2, but the problem remains largely unsolved.

### 1.1 Explainable lung cancer diagnoses

DL-based computer-aided diagnosis (CAD) systems have largely failed to be adopted into routine clinical work-flows. Unlike detection tasks, diagnosis (classification) requires radiologists to explain their predictions through the language of high-level visual attributes, shown in Fig. 1. For DL-powered CAD systems to be adopted by the healthcare industry and other high-risk domains, methods must be developed which can provide this same level of explainability. Towards this goal, we propose a novel multi-task deep capsule-based architecture for learning visually-interpretable feature representations within the vectors of the capsules. Although the proposed method is generic and it can be applied to many computer vision problems, we focus here on a high impact healthcare problem: lung cancer diagnosis.

Lung cancer is the far-leading cause of cancer-related death in both men and women [6]. The National Lung Screening Trial showed that screening patients with low-dose computed tomography (CT) has reduced lung cancer mortality by 20% [7, 8]. However, only 16% of lung cancer cases are diagnosed at an early stage [9]. The reasons behind this are due to the screening related challenges, including (a) high false positive rates, (b) over-diagnosis, and (c) missed nodules (i.e., tumor) during screening [10]. Based on DL models such as 2D and 3D deep convolutional neural networks (CNN), there have been several studies conducted to alleviate these challenges [11, 12, 13, 14, 15, 16, 17, 18, 19, 20, 21], and such explorations were partially successful in improving both nodule detection and image-based diagnostic rates. Noticeably, some achieved highly successful diagnosis results, comparable to or even better than expert level diagnosis [15]. Nevertheless, the black-box nature of these previous studies contributed to these methods not making their way into clinical routines. The purpose of this study is therefore to fill this important research gap by creating explainable medical diagnoses through learning visually-interpretable features from medical images with new DL models, specifically novel capsule network architectures.

### 1.2 Capsule neural networks and their visually-interpretable features

Capsule networks differ from traditional CNNs by replacing the scalar feature maps with vectorized representations, where these vectors are responsible for encoding orientation information, and thus provide equivariance to affine transformations on the input (as opposed to CNNs which are only equivariant to translation). These capsule vectors are then used in a dynamic routing algorithm which seeks to maximize the agreement between low-level and high-level features, not only in presence, but also in part-whole relationship agreement. In their introductory work [2], a capsule network (CapsNet) was shown to produce promising results on both the MNIST [22] and CIFAR10 [23] data sets; but more importantly, CapsNet was shown to encode high-level visually-interpretable feature representations of digits in MNIST (e.g. stroke thickness, skew, localized-parts) within the dimensions of its capsule vectors. While capsule networks are still a young area of research with many improvements to be made in terms of performance and accuracy, their ability to capture visually-interpretable features can be paramount in critical application domains that demand explainability of models.

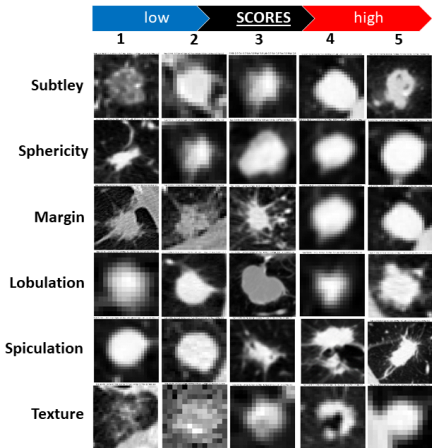


Figure 1: Lung nodules with high-level visual attribute scores as determined by expert radiologists. Scores were given from 1 – 5 for six different visual attributes related to diagnosing lung cancer.

### 1.3 Summary of our contributions

In this work, we introduce two novel multi-task capsule network architectures, providing explainable diagnoses in the same form as radiologists by learning to approximate six high-level visual attributes from lung nodules, as seen in Fig. 1, which radiologists estimate when determining the malignancy of a nodule. Additionally, our networks both segment nodules and determine their malignancy score in a multi-task learning (MTL) approach. Our first proposed architecture, called *X-Caps*, is an intuitive extension of the original CapsNet, where each dimension of the output capsule layer is supervised by a visual attribute label from multiple radiologists. By *forcing* each dimension of the capsule vector output to embed a specific visually-interpretable feature, a significant benefit (explainable decision) is obtained by unraveling knowledge hierarchy inside deep networks. The multiple visual attributes are learned simultaneously with their associated weights being updated by both the radiologists visual interpretation scores as well as their contribution to the final malignancy score, and the segmentation reconstruction error. This first network proved too restrictive and provides reaffirmation that deep features carry more discriminative power than these interpretable ones.

Our second architecture, called *DX-Caps*, is a much deeper capsule network with branching shared-weight paths for visual attribute and malignancy prediction. *DX-Caps* utilizes the recently introduced locally-constrained dynamic routing algorithm [24] and a novel capsule-average pooling (CAP) layer to reduce the spatial dimension of each capsule type. CAP recombines their vectors in a manner far-more computationally efficient than the fully-connected capsules used by the conventional CapsNet, similar to using global average pooling in a traditional CNN. These novelties allowed for the creation of a much deeper capsule network while keeping the memory to a single 12 GB GPU. *DX-Caps* malignancy predictive performance (without any pre-training) is on par with previously state-of-the-art deep pre-trained 2D/3D CNN works (e.g. [13, 14]), while also outputting visual attribute scores, where nearly no previous works do so.

Furthermore, since radiologists' scores vary significantly between each other for both malignancy and visual characteristics of a given nodule, it is not possible to train the proposed networks directly against these scores. Previous works train against the mean of the radiologist scores and convert the mean to a binary label (malignant or benign). However, this throws away significant information. In our proposed method, we fit a Gaussian distribution of mean and variance equal to that of the radiologists' scores for a given nodule and compute the mean squared error between this and our network output for supervised training. In this way, overconfidence by the network on more ambiguous nodules is punished in proportion to radiologists' disagreement, and likewise for under-confidence and strong radiologist agreement. This allows our method to produce classification scores across all five possible score values, rather than simply binary labels as in previous studies.

The rest of the paper is organized as follows. In Section 2, we summarize related works in the literature pertaining to interpretable deep learning, lung cancer diagnosis using deep networks, and capsule networks in medical imaging. In Section 3, we introduce our proposed paradigm of learning visually-interpretable features via our newly designed deep multi-task capsule networks. In Section 4, we explain the our experiments and results. We conclude our work with discussions in Section 5.

## 2 Related work

The majority of work in explainable deep learning has focused around *post hoc* deconstruction of already trained models. Two main approaches are primarily investigated, interpretation of the features learned by the networks and explaining deep networks' final predictions, at both the local (*i.e.* individual neurons) and global (*i.e.* entire layers/networks) level. These approaches typically rely on human-experts to examine their results and attempt to discover meaningful patterns. While there are numerous studies on explainable deep learning, we will attempt to faithfully cover the more prominent approaches. Following this, Section 2 will cover relevant lung cancer diagnosis and capsule-based works.

**Visualization of features** Several works have attempted to examine network interpretability at the individual neuron level. Some of the earliest methods focused on visualizing individual filters and activation maps. While this can provide some insight into certain aspects of a network, such as dead neurons, the visualization of individual filters or feature maps are typically not interpretable at the human-level. Zeiler and Fergus [25] attached a deconvolutional network to network layers

to map activations back to pixel space for visualization. Later, Springenberg *et al.* [26] used an all convolutional network and a guided-backpropagation algorithm to create much sharper visualizations which did not require the keys of the pooling operations. Mahendran and Vedaldi [27] focused more on layers of neurons and examine the representations learned by shallow and deep CNNs by inverting images using gradient descent. While these methods provide some insight into what CNNs learn, they are ultimately limited, as deep networks typically have hundreds of thousands of neurons and it is intractable to visually examine all or even large subsets of neurons in a network. Additionally, there is evidence to suggest these visualizations are unrelated to network predictions [28].

**Receptive fields, input contributions** Beyond visualizing the features of CNNs, several methods have attempted to examine the effect of individual neurons or image regions on network outputs. In this first category, Girshick *et al.* [29] examined the receptive field of individual neurons and found the images which maximally activated each. Kindermans *et al.* [30] showed that [26, 25] (discussed above) did not create theoretically correct explanations for linear models, and created PatternNet and PatternAttribution to better visualize neuron activations. In the latter category, Kumar *et al.* [31] examined which input region correspond most strongly with each output class. An occlusion-based approach was used by Zeiler and Fergus [25] for masking out image regions to examine their contribution to the final output. One of the most popular methods of visualizing input contributions is Grad-CAM [32] which highlights the relative positive activation map of convolutional layers with respect to network outputs. Arguably, saliency detection can also fall into this category of determining which input regions are important. While these methods give important information related to designing networks and training data, they tell us very little about the internal representations being learned.

**Feature spaces and GANs** Rather than looking at the individual neurons or image regions, several approaches instead focus on examining the feature spaces learned by deep networks. Generative adversarial networks (GAN) by Goodfellow *et al.* [33], show vulnerable regions of a learned feature space for a given network. In [34], Chen *et al.* creates a GAN-based method called InfoGAN to separate noise from the “latent code” in images. Using this method, they maximize the mutual information between the latent representations and the image inputs, encoding concepts such as rotation, width, and digit type for MNIST. In a similar way, capsule networks by Sabour *et al.* [2] (CapsNet) encode visually-interpretable concepts such as stroke thickness, skew, rotation, and others. These two methods are the most similar to the proposed approach. Lakkaraju *et al.* [35] attempt to discover a CNN’s “blind spots” by sampling points in feature space in a weakly-supervised manner. While the other methods mentioned can provide some important clues about the feature space being learned, InfoGAN and CapsNet show the most promise for encoding and extracting visually-interpretable features.

**Disentangling representations** Methods for disentangling representations are focused on discovering the visual patterns learned by CNN filters, then disentangling their relationship to each other. Zhang *et al.* [36] created multi-layer graph structure, where each layer of the graph matches each layer of the CNN. Activated visual patterns across all training images are added as nodes and patterns which co-occur in images have edges added between them. In [37], Bau *et al.* introduced six types of semantic filters for CNNs: objects, parts, scenes, textures, materials, and colors. Networks are then trained using these labels at the pixel-level to identifies hidden units’ semantics for any given CNN, and align them with human-interpretable concepts. Unfortunately, the former of these methods can only provide little about the features learned, while the latter method requires a dramatic increase in labeled data, where multiple labels need to be provided at the pixel level.

**Lung nodule classification** The majority of recent lung cancer diagnosis (nodule classification) studies have focused on deep 2D, multi-view, and 3D CNNs, with most works trained/tested on the publicly available LIDC-IDRI data set from Lung Image Database Consortium [38]. Buty *et al.* [13] extracted features from a pre-trained 2D multi-view CNN while encoding shape information through spherical harmonics (SH) to improve diagnostic accuracy from 79% (CNN) to 82% (CNN+SH). Hussein *et al.* [14] achieved a similar result, extracting deep features from a multi-view CNN then applying a Gaussian process regression strategy to achieve 82% accuracy. In a later work, Hussein *et al.* [15] reported a deep 3D CNN, pre-trained on Sports-1M [39], used in a MTL with trace norm approach to combine visual attributes achieved 80% accuracy. In this same work, the authors propose a more complicated regularized graphical lasso post-processing algorithm to combine imaging

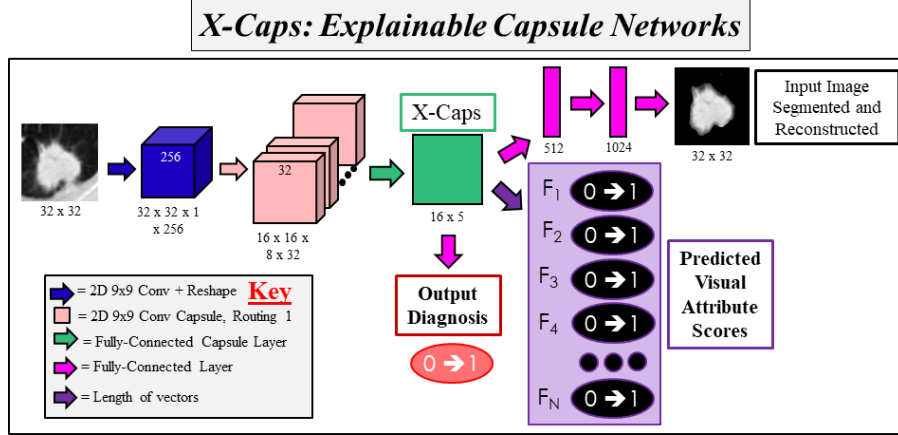


Figure 2: X-Caps: Explainable Capsule Networks. For a screen detected nodule, the proposed network (1) predicts high-level visual attributes of the nodule, (2) segment the nodule and reconstruct the input image, and (3) classify nodule as malignant or benign.

features with radiologists’ visual attributes and gained an 11% accuracy improvement; however, no results were reported on the visual attribute predictions. Shen *et al.* [1] is one of the only works in the literature to attempt to create an interpretable framework by simultaneously predicting visual attribute scores along with malignancy. The authors used a deep multi-path dense 3D CNN to achieve an accuracy of 84%, however their results on individual attribute predictions were as low as 55%. Most recently, some deeper multi-crop [40], multi-scale [41], and denser multi-path multi-output [42] CNNs, using methods such as curriculum learning [43] or gradient boosting machines [44] and complicated post-processing techniques [15], have been applied to push diagnosis accuracy to 87% – 92%. However, adding such techniques is beyond the scope of this work and would lead to an unwieldy enumeration of ablation studies necessary to understand the contributions between our proposed capsule architectures and such techniques. For a fair comparison in this study, we compare our method directly against CapsNet and CNNs without post-processing techniques.

**Capsule network-based medical diagnosis** It is also worth noting, a number of recent studies have proposed using CapsNet for a variety of medical imaging classification tasks [45, 46, 47], although no work in the literature has studied capsule networks for lung cancer diagnosis. Nonetheless, since these methods nearly all follow the exact CapsNet architecture, or propose minor modifications which produce nearly identical predictive performance [48], it is sufficient to compare only with CapsNet in reference to these works. Lastly, a recent study by Duarte *et al.* [49] proposed a network which performed action recognition and localization in videos. However, since this network only contains two capsule layers inside a deep 3D CNN, whereas our proposed architectures contain nearly all capsule layers, we do not compare with this work.

### 3 Learning visually-interpretable features

The goal of our proposed method is to model visual attributes using capsule neural networks in order to provide the same explanations as radiologists for predicting malignancy, while simultaneously performing malignancy prediction and nodule segmentation/reconstruction. The Lung Image Database Consortium and Image Database Resource Initiative (LIDC-IDRI) [38], contains a collection of lung nodules with scores ranging from 1 – 5 across a set of visual attributes, indicating their relative appearance, and malignancy, as scored by up to four radiologists. These characteristics and scores are shown in Figure 1.

#### 3.1 Capsules for encoding visual attributes

Our first approach, referred to as *explainable capsules*, or *X-Caps*, was designed to remain as similar as possible to CapsNet, while allowing us to have more control over the visually-interpretable features

learned by the capsule vectors. CapsNet already showed great promise when trained on the MNIST data set for its ability to model high-level visually-interpretable features. With this first study, we examine the ability of capsules to model *specific* visual attributes within their vectors, rather than simply hoping some are learned successfully in the more challenging lung nodule data. As shown in Figure 2, X-Caps shares the same overall structure as CapsNet, with the major difference being the addition of the supervised labels being provided for each dimension of the X-Caps vectors. To compute a final malignancy score, we attach a fully-connected layer to all six of these vectors with a Sigmoid activation. For X-Caps, all output labels have their values scaled to  $[0, 1]$  to allow for easier training with the activation functions.

As in CapsNet, we also perform reconstruction of the input as a form of regularization. However, we extend the idea of regularization to perform a sudo-segmentation. Whereas in segmentation, the goal is to output a binary mask of pixels which belong to the nodule region, in our formulation we attempt to reconstruct only the pixels which belong to the nodule region, while the rest are mapped to zero. More specifically, we formulate this problem as

$$R^{x,y} = I^{x,y} \times S^{x,y} \mid S^{x,y} \in \{0, 1\}, \text{ and} \quad (1)$$

$$\mathcal{L}_R = \frac{\gamma}{X \times Y} \sum_x^X \sum_y^Y \|R^{x,y} - O_r^{x,y}\|, \quad (2)$$

where  $\mathcal{L}_R$  is the supervised loss for the reconstruction regularization,  $\gamma$  is a weighting coefficient for the reconstruction loss,  $R^{x,y}$  is the reconstruction target pixel,  $S^{x,y}$  is the ground-truth segmentation mask value, and  $O_r^{x,y}$  is the output of the reconstruction network, at pixel location  $(x, y)$ , respectively, and  $X$  and  $Y$  are the width and height, respectively, of the input image. This adds another task to our MTL approach and an additional supervisory signal which can help our network distinguish visual characteristics from background noise. The malignancy prediction score, as well as each of the visual attribute scores also provide a supervisory signal in the form of

$$\mathcal{L}_a = \sum_n^N \alpha^n \|A^n - O_a^n\| \text{ and } \mathcal{L}_m = \beta \|M - O_m\|, \quad (3)$$

where  $\mathcal{L}_a$  is the combined loss for the visual attributes,  $A^n$  is the average of the attribute scores given by at minimum three radiologists for attribute  $n$ ,  $N$  is the total number of attributes,  $\alpha^n$  is the weighting coefficient placed on the  $n^{th}$  attribute,  $O_a^n$  is the network prediction for the score of the  $n^{th}$  attribute,  $\mathcal{L}_m$  is the loss for the malignancy score,  $M$  is the average of the malignancy scores given by at minimum three radiologists,  $O_m$  is the network prediction for the average malignancy score, and  $\beta$  is the weighting coefficient for the malignancy score. In this way, the overall loss for X-Caps is simply  $\mathcal{L} = \mathcal{L}_m + \mathcal{L}_a + \mathcal{L}_R$ . For simplicity, the values of each  $\alpha^n$  and  $\beta$  are set to 1, and  $\gamma$  is set to 0.384<sup>1</sup>.

### 3.2 Going deeper with explainable capsules

We hypothesize that the lung nodules and visual attributes being studied would be more complex in nature than handwritten digits and require a deeper hierarchical structure to better represent them. While X-Caps provides some empirical evidence towards the ability for capsule vectors to have their vectors explicitly supervised to learn specific visual attributes, we push the network deeper and study a more complex network structure, while relaxing the requirement to use *only* visually-explainable features in malignancy prediction. Building on the locally-constrained dynamic routing introduced by LaLonde and Bagci [24], and with our newly proposed capsule-average pooling (CAP), we are able to create a deep network structure which we call *DX-Caps*, or *deep explainable capsules*.

The proposed *DX-Caps*, illustrated in Figure 3, consists of a single convolutional layer, followed by five capsule layers before branching into separate paths for predicting malignancy and visual attributes. With this structure, each visual attribute and malignancy have their own capsule types. This

<sup>1</sup> Further tuning of these parameters could potentially lead to superior results but we did not have the computational resources to perform such an analysis for this study.

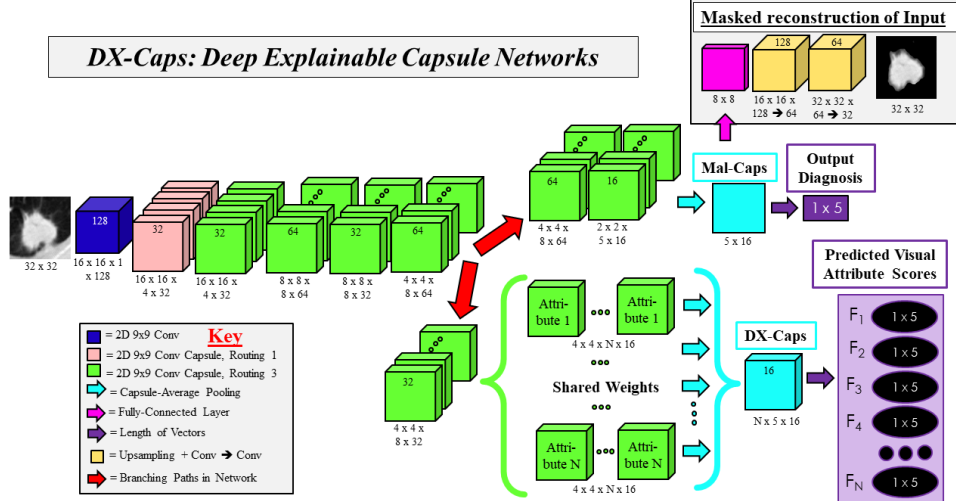


Figure 3: *DX-Caps*: Deep Explainable Capsule Network. Similar to the *X-Caps*, the proposed network (1) predicts high-level visual attributes of the nodule, (2) segments the nodule through a masked reconstruct the input image, and (3) classifies nodules scores on a scale of 1 – 5. The newly proposed capsule-average pooling allows us to create very deep networks while performing classification.

allows to network to encode and predict high-level visual attribute information to a greater degree, as for a given attribute, each score has its own vector, where the vector being used for attribute  $n$  score 0 is different from the vector used to identify attribute  $n$  score 5. Since these weights are shared, we force the capsule vectors to jointly learn to encode orientation information about all visual attributes in each of these capsule types, while capsules before the branching learn features relevant to both visual attribute and malignancy prediction from our MTL loss function.

For a deeper capsule network, there was a need to replace the fully-connected capsule layer used by CapsNet, which was far too memory intensive to be computationally tractable in single GPU training. To this end, we introduce a capsule-average pooling (CAP) algorithm which splits apart capsules by capsule type in a given layer and reforms new capsules as the average of the vectorized activations from the previous layer. More formally, for any given layer  $\ell_i$ , there exists a set of capsule types  $C = \{c_1, c_2, \dots, c_n \mid n \in \mathbb{N}\}$ , and within each capsule type, there exists a  $2D$  grid of capsule vectors  $V = \{v_{1,1}, \dots, v_{1,w}, \dots, v_{h,1}, \dots, v_{h,w}\}$ , where  $h \times w$  is the spatial dimensions of the capsule type at layer  $\ell$ . Each  $v$  has dimension  $1 \times a$  such that  $a$  is the length of the capsule vectors. Parent capsules are formed by computing the average across the spatial grid along each dimension of the capsule vectors,  $v$ . Therefore each child capsule in  $C$  has exactly one corresponding parent capsule, where the set of parents capsules is denoted as  $P = \{p_1, p_2, \dots, p_m \mid m \in \mathbb{N}\}$ . For each  $p \in P$ , we compute the following  $p_i = \frac{1}{w \times h} \sum_x^w \sum_y^h v_{x,y}$ , where each  $p_i$  now have dimension  $1 \times a$ . A single overall parent capsule is formed by concatenating each  $p_i$  to form a  $2D$  vector of dimension  $m \times a$ . In the case of our proposed *DX-Caps*,  $m$  is the number of score classes we have, *i.e.* five. The output is then formed as normal by computing the length of each vector in this  $2D$  grid to arrive at a final  $m$  values corresponding to our classification prediction. This formulation reduces the parameter and memory burden and allows us to create *DX-Caps* while still fitting into a single 12GB GPU's memory.

**Uncertainty modeling of the visual scoring** All previous works in lung nodule classification follow the same strategy of averaging radiologists' scores for visual attributes and malignancy. To better model the uncertainty inherently present in the labels due to inter-observer variation, we propose a different approach: rather than simply trying to regress the average of the values submitted by radiologists, or performing binary classification of these values rounded as above or below the score of 3, we attempt to predict the *distribution* of radiologists' scores. Specifically, for a given nodule where we have at minimum three radiologists' score values for each attribute and for malignancy prediction, we compute the mean and standard deviation of those values and fit a Gaussian function to them, which is in turn used as the ground-truth for our classification vector. Nodules with strong

inter-observer agreement produce a sharp peak, in which case wrong or unsure (*i.e.* low confidence score) predictions are severely punished. Likewise, for low inter-observer agreement nodules, we expect our network to output a more spread distribution and it will be punished for strongly predicting a single class label. This proposed approach allows us to model the uncertainty present in radiologists’ labels in a way that no previous study has.

## 4 Experiments and results

For our experiments, we used publicly available LIDC-IDRI data set [38]. Five-fold stratified cross-validation was performed to split the nodules into training and testing sets, with 10% of each training set set aside for validation and early stopping. All models were trained using Adam [50] with an initial learning rate of 0.001 reduced by a factor of 0.1 after validation loss plateau. All code is implemented in Keras with TensorFlow backend support and will be made publicly available. Consistent with the literature, predictions were considered correct if within 1.0 of the radiologists’ average score.

The experimental results summarized in Table 1 illustrate the prediction of visual attributes with the proposed X-Caps and DX-Caps in comparison with a adapted version CapsNet and a deep multi-path dense 3D CNN (HSCNN [1]). To the best of our knowledge, HSCNN is the only other work in the literature which presents attribute-level results pursuant to learning interpretable features through the modeling of high-level visual attributes for lung cancer diagnosis. *DX-Caps* outperformed baseline CapsNet as well as *X-Caps* in predicting both malignancy and visual attribute scores. While HSCNN slightly outperformed *DX-Caps* in malignancy prediction, it performed significantly worse than *DX-Caps* on average at attribute prediction, which is the main focus for explainability of predictions to radiologists. Experimental results support our hypothesis that a deep capsule network, through the aid of the introduced capsule-average pooling, can model visual attributes better than a baseline X-Caps, CapsNet, and a dense CNN.

Table 1: Prediction accuracy of visual attribute learning with capsule networks. While HSCNN, a multi-path dense 3D CNN, predicts malignancy at a slightly higher accuracy, it performs significantly worse than *DX-Caps* at attribute prediction, which is the main focus for explainability. It is worth noting that margin and lobulation have a lower correlation with malignancy than nearly all other attributes [51], and this might in part explain *DX-Caps* lower accuracy on these attributes.

Prediction Accuracy Attributes	Capsule Networks			CNNs
	CapsNet	X-Caps	DX-Caps	HSCNN [1]
subtlety	-	83.0%	83.0%	71.9%
sphericity	-	76.8%	97.5%	55.2%
margin	-	78.7%	70.2%	72.5%
lobulation	-	25.6%	70.2%	-
spiculation	-	37.8%	75.4%	-
texture	-	90.0%	90.0%	83.4%
<b>Malignancy</b>	78.32%	69.41%	80.17%	84.20%

## 5 Discussions and concluding remarks

Deep leaning-generated predictions are mostly black-box in nature and not explainable; hence, not trusted by healthcare specialists. Available studies for explaining DL models, typically focus on *post hoc* interpretations of trained networks, rather than attempting to build-in explainability. This is the first study, to the best of our knowledge, for learning to encode high-level visual attributes from radiologists within the vectors of a capsule-based network to perform explainable image-based diagnosis. We simultaneously approximate visually-interpretable attributes along with malignancy predictions through individual capsule types in order to explain these malignancy predictions in the same language as radiologists. The results of our study show the proposed deep explainable capsule architecture, *DX-Caps*, made possible by introducing a capsule-average pooling function, successfully approximated visual attribute scores far better than a deep multi-path dense 3D CNN. We also implemented a version of CapsNet for lung cancer diagnosis for the first time in the literature and a shallow version of our explainable capsule network, *X-Caps*, with both achieving inferior performance as compared with *DX-Caps*. As the field of capsule networks progress and



similar advancements such as those made with CNNs (*e.g.* residual/dense connections, batch/group normalization), deeper and more powerful capsule networks can be created to boost performance even further.

## References

- [1] Shiwen Shen, Simon X Han, Denise R Aberle, Alex A Bui, and William Hsu. An interpretable deep hierarchical semantic convolutional neural network for lung nodule malignancy classification. *Expert Systems with Applications*, 2019.
- [2] Sara Sabour, Nicholas Frosst, and Geoffrey E Hinton. Dynamic routing between capsules. In *Advances in Neural Information Processing Systems*, pages 3856–3866, 2017.
- [3] Jason Bloomberg. Don’t Trust Artificial Intelligence? Time To Open The AI ‘Black Box’. <http://www.forbes.com/sites/jasonbloomberg/2018/09/16/dont-trust-artificial-intelligence-time-to-open-the-ai-black-box/#6ceaf3793b4a>, 11.16.2018. Forbes Magazine.
- [4] Marianne Lehnis. Can We Trust AI If We Don’t Know How It Works? <http://www.bbc.com/news/business-44466213>, 15.06.2018. BBC News.
- [5] Vyacheslav Polonski. People Don’t Trust AI—Here’s How We Can Change That. <http://www.scientificamerican.com/article/people-dont-trust-ai-heres-how-we-can-change-that/>, 10.01.2018. Scientific American.
- [6] National Center for Health Statistics (US et al. Health, united states, 2016: with chartbook on long-term trends in health, 2017.
- [7] National Lung Screening Trial Research Team. Reduced lung-cancer mortality with low-dose computed tomographic screening. *New England Journal of Medicine*, 365(5):395–409, 2011.
- [8] David F Yankelevitz and James P Smith. Understanding the core result of the national lung screening trial. *New England Journal of Medicine*, 368(15):1460–1461, 2013.
- [9] N Howlander, AM Noone, M Krapcho, D Miller, K Bishop, SF Altekruse, CL Kosary, M Yu, J Ruhl, Z Tatalovich, A Mariotto, DR Lewis, HS Chen, EJ Feuer, and KA Cronin. SEER Cancer Statistics Review, 1975-2013, National Cancer Institute. [https://seer.cancer.gov/archive/csr/1975\\_2013/](https://seer.cancer.gov/archive/csr/1975_2013/), 04.2018.
- [10] Henry M Marshall, Rayleen V Bowman, Ian A Yang, Kwun M Fong, and Christine D Berg. Screening for lung cancer with low-dose computed tomography: a review of current status. *Journal of thoracic disease*, 5(Suppl 5):S524, 2013.
- [11] Hoo-Chang Shin, Holger R Roth, Mingchen Gao, Le Lu, Ziyue Xu, Isabella Noguees, Jianhua Yao, Daniel Mollura, and Ronald M Summers. Deep convolutional neural networks for computer-aided detection: Cnn architectures, dataset characteristics and transfer learning. *IEEE transactions on medical imaging*, 35(5):1285–1298, 2016.
- [12] Arnaud Arindra Adiyoso Setio, Alberto Traverso, Thomas De Bel, Moira SN Berens, Cas van den Bogaard, Piergiorgio Cerello, Hao Chen, Qi Dou, Maria Evelina Fantacci, Bram Geurts, et al. Validation, comparison, and combination of algorithms for automatic detection of pulmonary nodules in computed tomography images: the luna16 challenge. *Medical image analysis*, 42:1–13, 2017.
- [13] Mario Buty, Ziyue Xu, Mingchen Gao, Ulas Bagci, Aaron Wu, and Daniel J Mollura. Characterization of lung nodule malignancy using hybrid shape and appearance features. In *International Conference on Medical Image Computing and Computer-Assisted Intervention*, pages 662–670. Springer, 2016.
- [14] Sarfaraz Hussein, Robert Gillies, Kunlin Cao, Qi Song, and Ulas Bagci. Tumornet: Lung nodule characterization using multi-view convolutional neural network with gaussian process. In *Biomedical Imaging (ISBI 2017), 2017 IEEE 14th International Symposium on*, pages 1007–1010. IEEE, 2017.
- [15] Sarfaraz Hussein, Kunlin Cao, Qi Song, and Ulas Bagci. Risk stratification of lung nodules using 3d cnn-based multi-task learning. In *International Conference on Information Processing in Medical Imaging*, pages 249–260. Springer, 2017.
- [16] Naji Khosravan and Ulas Bagci. S4nd: Single-shot single-scale lung nodule detection. *MICCAI*, 2018.
- [17] Naji Khosravan, Haydar Celik, Baris Turkbey, Elizabeth Jones, Bradford Wood, and Ulas Bagci. A collaborative computer aided diagnosis (c-cad) system with eye-tracking, sparse attentional model, and deep learning. *Medical Image Analysis*, 2019.
- [18] Arnaud Arindra Adiyoso Setio, Francesco Ciompi, Geert Litjens, Paul Gerke, Colin Jacobs, Sarah J van Riel, Mathilde Marie Winkler Wille, Matiullah Naqibullah, Clara I Sánchez, and Bram van Ginneken. Pulmonary nodule detection in ct images: false positive reduction using multi-view convolutional networks. *IEEE transactions on medical imaging*, 35(5):1160–1169, 2016.

- [19] Xiaojie Huang, Junjie Shan, and Vivek Vaidya. Lung nodule detection in ct using 3d convolutional neural networks. In *Biomedical Imaging (ISBI 2017), 2017 IEEE 14th International Symposium on*, pages 379–383. IEEE, 2017.
- [20] Jia Ding, Aoxue Li, Zhiqiang Hu, and Liwei Wang. Accurate pulmonary nodule detection in computed tomography images using deep convolutional neural networks. In *International Conference on Medical Image Computing and Computer-Assisted Intervention*, pages 559–567. Springer, 2017.
- [21] Qi Dou, Hao Chen, Lequan Yu, Jing Qin, and Pheng-Ann Heng. Multilevel contextual 3-d cnns for false positive reduction in pulmonary nodule detection. *IEEE Transactions on Biomedical Engineering*, 64(7):1558–1567, 2017.
- [22] Yann LeCun, Léon Bottou, Yoshua Bengio, and Patrick Haffner. Gradient-based learning applied to document recognition. *Proceedings of the IEEE*, 86(11):2278–2324, 1998.
- [23] Alex Krizhevsky. Learning multiple layers of features from tiny images. Technical report, Citeseer, 2009.
- [24] Rodney LaLonde and Ulas Bagci. Capsules for object segmentation. *arXiv preprint arXiv:1804.04241*, 2018.
- [25] Matthew D Zeiler and Rob Fergus. Visualizing and understanding convolutional networks. In *European conference on computer vision*, pages 818–833. Springer, 2014.
- [26] Jost Tobias Springenberg, Alexey Dosovitskiy, Thomas Brox, and Martin Riedmiller. Striving for simplicity: The all convolutional net. *arXiv preprint arXiv:1412.6806*, 2014.
- [27] Aravindh Mahendran and Andrea Vedaldi. Understanding deep image representations by inverting them. In *Proceedings of the IEEE conference on computer vision and pattern recognition*, pages 5188–5196, 2015.
- [28] Weili Nie, Yang Zhang, and Ankit Patel. A theoretical explanation for perplexing behaviors of backpropagation-based visualizations. In *International Conference on Machine Learning*, pages 3806–3815, 2018.
- [29] Ross Girshick, Jeff Donahue, Trevor Darrell, and Jitendra Malik. Rich feature hierarchies for accurate object detection and semantic segmentation. In *Proceedings of the IEEE conference on computer vision and pattern recognition*, pages 580–587, 2014.
- [30] Pieter-Jan Kindermans, Kristof T Schütt, Maximilian Alber, Klaus-Robert Müller, Dumitru Erhan, Been Kim, and Sven Dähne. Learning how to explain neural networks: Patternnet and patternattribution. In *International Conference on Learning Representations (ICLR)*, 2018.
- [31] Devinder Kumar, Alexander Wong, and Graham W Taylor. Explaining the unexplained: A class-enhanced attentive response (clear) approach to understanding deep neural networks. In *IEEE Computer Vision and Pattern Recognition (CVPR) Workshop*, 2017.
- [32] Ramprasaath R Selvaraju, Michael Cogswell, Abhishek Das, Ramakrishna Vedantam, Devi Parikh, and Dhruv Batra. Grad-cam: Visual explanations from deep networks via gradient-based localization. In *Proceedings of the IEEE International Conference on Computer Vision*, pages 618–626, 2017.
- [33] Ian Goodfellow, Jean Pouget-Abadie, Mehdi Mirza, Bing Xu, David Warde-Farley, Sherjil Ozair, Aaron Courville, and Yoshua Bengio. Generative adversarial nets. In *Advances in neural information processing systems*, pages 2672–2680, 2014.
- [34] Xi Chen, Yan Duan, Rein Houthoofd, John Schulman, Ilya Sutskever, and Pieter Abbeel. Infogan: Interpretable representation learning by information maximizing generative adversarial nets. In *Advances in neural information processing systems*, pages 2172–2180, 2016.
- [35] Himabindu Lakkaraju, Ece Kamar, Rich Caruana, and Eric Horvitz. Identifying unknown unknowns in the open world: Representations and policies for guided exploration. In *AAAI*, pages 2124–2132, 2017.
- [36] Quanshi Zhang, Ruiming Cao, Feng Shi, Ying Nian Wu, and Song-Chun Zhu. Interpreting cnn knowledge via an explanatory graph. In *AAAI*, 2018.
- [37] D. Bau, B. Zhou, A. Khosla, A. Oliva, and A. Torralba. Network dissection: Quantifying interpretability of deep visual representations. In *2017 IEEE Conference on Computer Vision and Pattern Recognition (CVPR)*, volume 00, pages 3319–3327, July 2017.
- [38] S.G Armato III, G. McLennan, L. Bidaut, M. F McNitt-Gray, C. R Meyer, A. P Reeves, B. Zhao, D. R Aberle, C. I Henschke, E. A Hoffman, et al. The Lung Image Database Consortium (LIDC) and Image Database Resource Initiative (IDRI): a completed reference database of lung nodules on CT scans. *Medical Physics*, 38(2):915–931, 2011.
- [39] Andrej Karpathy, George Toderici, Sanketh Shetty, Thomas Leung, Rahul Sukthankar, and Li Fei-Fei. Large-scale video classification with convolutional neural networks. In *Proceedings of the IEEE conference on Computer Vision and Pattern Recognition*, pages 1725–1732, 2014.

- [40] Wei Shen, Mu Zhou, Feng Yang, Dongdong Yu, Di Dong, Caiyun Yang, Yali Zang, and Jie Tian. Multi-crop convolutional neural networks for lung nodule malignancy suspiciousness classification. *Pattern Recognition*, 61:663–673, 2017.
- [41] Wei Shen, Mu Zhou, Feng Yang, Caiyun Yang, and Jie Tian. Multi-scale convolutional neural networks for lung nodule classification. In *International Conference on Information Processing in Medical Imaging*, pages 588–599. Springer, 2015.
- [42] Raunak Dey, Zhongjie Lu, and Yi Hong. Diagnostic classification of lung nodules using 3d neural networks. In *2018 IEEE 15th International Symposium on Biomedical Imaging (ISBI 2018)*, pages 774–778. IEEE, 2018.
- [43] Aiden Nibali, Zhen He, and Dennis Wollersheim. Pulmonary nodule classification with deep residual networks. *International journal of computer assisted radiology and surgery*, 12(10):1799–1808, 2017.
- [44] Wentao Zhu, Chaochun Liu, Wei Fan, and Xiaohui Xie. Deeplung: Deep 3d dual path nets for automated pulmonary nodule detection and classification. In *2018 IEEE Winter Conference on Applications of Computer Vision (WACV)*, pages 673–681. IEEE, 2018.
- [45] Parnian Afshar, Arash Mohammadi, and Konstantinos N Plataniotis. Brain tumor type classification via capsule networks. In *2018 25th IEEE International Conference on Image Processing (ICIP)*, pages 3129–3133. IEEE, 2018.
- [46] Tomas Iesmantas and Robertas Alzbutas. Convolutional capsule network for classification of breast cancer histology images. In *International Conference Image Analysis and Recognition*, pages 853–860. Springer, 2018.
- [47] Yan Shen and Mingchen Gao. Dynamic routing on deep neural network for thoracic disease classification and sensitive area localization. In *International Workshop on Machine Learning in Medical Imaging*, pages 389–397. Springer, 2018.
- [48] Aryan Mobiny and Hien Van Nguyen. Fast capsnet for lung cancer screening. In *International Conference on Medical Image Computing and Computer-Assisted Intervention*, pages 741–749. Springer, 2018.
- [49] Kevin Duarte, Yogesh Rawat, and Mubarak Shah. Videocapsulenet: A simplified network for action detection. In *Advances in Neural Information Processing Systems*, pages 7610–7619, 2018.
- [50] Diederik P Kingma and Jimmy Ba. Adam: A method for stochastic optimization. *arXiv preprint arXiv:1412.6980*, 2014.
- [51] Xiuli Li, Yueying Kao, Wei Shen, Xiang Li, and Guotong Xie. Lung nodule malignancy prediction using multi-task convolutional neural network. In *Medical Imaging 2017: Computer-Aided Diagnosis*, volume 10134, page 1013424. International Society for Optics and Photonics, 2017.